Academic Science Journal

Structural, Optical and Electrical Properties of (PbS: Co) Nanostructured Thin Films Synthesized by Pulsed Laser Ablation Deposition Technique

Nawar T. Mohammed*[1], Jassim M. Mansour and Kadhim A. Aadim[2]

[1]Department of Physics – College of Science – University of Diyala – Diyala, Iraq
[2]Department of Physics – College of Science – University of Baghdad – Baghdad, Iraq

basicsci14@uodiyala.edu.iq

Received: 28 May 2022 **Accepted: 13 July 2022**

DOI: https://dx.doi.org/10.24237/ASJ.01.01.592C

Abstract

In the present work, thin films of Lead sulphide (PbS) and different mixing ratios of Co (30%, 50% and 70%) were prepared by (PLD) technique at glass substrates at 1064nm wavelength with 600mj laser energy. The structural measurements were determined by X-ray diffraction studies for pure PbS and other mixing ratio . The present thin films were showed that the structure is face-centered-cubic. the grain size were found 17.74 nm for pure and increase to 31.3 and 55.67 nm when the mixing increase to 30% and 50% respectively and decreases to 39.57nm when mixed with 70% Co. The optical properties were measured at wavelength (300 - 1100) nm for PbS thin films. The absorption coefficient increases with increasing mixing ratio, The energy gap for pure PbS thin film was (2.43 ev) and increases to (2.54 ev) and then decreases to (2.42 ev) and (2.30 ev) with increasing of mixing ratio.

Keywords: Lead sulphide, pulsed laser Deposited, XRD diffraction, optical properties, Electrical properties.

Academic Science Journal

الخصائص التركيبية ، البصرية والكهربائية لاغشية (PbS:Co)نانوية التركيب المحضرة بطريقة الترسيب بالليزر النبضي

نوار ثامر محمد[1]، جاسم محمد منصور[1] وكاظم عبد الواحد عادم[2]

قسم الفيزياء – كلية العلوم – جامعة ديالى – ديالى، العراق

[2]قسم الفيزياء – كلية العلوم – جامعة بغداد – بغداد، العراق

الخلاصة

في البحث الحالي، حضرت اغشية كبريتيد الرصاص المخلوط مع نسب مختلفة (30% و50% و70%) من الكوبلت بتقنية الليزر النبضي باستخدام قواعد من الزجاج عند طول موجي 1064 نانومتر وبطاقة 600 ملي جول. تم قياس الخواص التركيبية بدراسة حيود الاشعة السينية لأغشية كبريتيد الرصاص النقي والمخلوط بالنسب الاخرى من الكوبلت حيث بين ان التركيب هو مكعب متمركز الوجه. وجد ان الحجم الحبيبي هو 17.74 نانو متر ويزداد بعد الخلط بنسبة 30% الى 51.30 ويزداد عند الخلط بنسبة 50% الى 55.67 ثم بعدها يقل الى 39.57 نانو متر عند الخلط بنسبة 70% من الكوبلت. قيست الخواص البصرية عند الطول الموجي (300-1100) نانو متر لكبريتيد الرصاص. يزداد معامل الامتصاص مع زيادة نسبة الخلط، فجوة الطاقة لأغشية كبريتيد الرصاص النقي (2.43) وتزداد الى (2.54) ثم بعدها تقل الى (2.42) ثم (2.30) بزيادة نسبة الخلط.

كلمات مفتاحية :كبريتيد الرصاص، الترسيب بالليزر النبضي، حيود الاشعة السينية، الخواص البصرية، الخواص الكهربائية

Introduction

Thin film polycrystalline semiconductors have sparked a lot of attention in recent years, and they've been used in a variety of electrical devices. The key driver of this interest is the cheap production costs [1]. Infrared detectors, transistors, photoconductive cells, high-temperature lubricants, and ceramic glazing all employ it. It's as highlighted also utilized to remove mercaptans from petroleum distillates as a catalyst in petroleum refining [2].

Lead Sulphide (PbS) semiconductor has a low band gap of 0.4 eV at room temperature [3]. Semiconductor materials now occupy high situated in the research and solid state technology and it is a IV-VI compound semiconductor . [4].

The band gap of PbS may be significantly change greatly by modifying the grain size, and it has been reported that lowering the grain size to the Nano regime can expand the band gap to as high as 2.5 eV from its bulk value. [5]. Optical band gap of PbS thin films may be tuned (1.5 eV) and electrical resistivity can be decreased by modifying various preparation conditions [6,7]. These characteristics have been linked to growth circumstances and substrate types. For these reasons, several research groups are interested in developing and studying this material by various deposition procedures such as electrode position, spray pyrolysis, photo accelerated chemical deposition microwave-heating, and chemical bath deposition (CBD) [8]. Pulsed laser deposition is one of the most recent and cutting-edge thin film deposition processes. Pulsed laser deposition (PLD) is one of the most recent and cutting-edge thin film deposition processes.

PLD is one of the most adaptable ways for obtaining layers of various materials that can be processed into a pellet target. One of essential features of this approach is the ability to keep the ablated target's stoichiometry in the deposited layer [9- 11]. PLD is more versatile than other traditional processes, allows for precise of film thickness control. Laser ablation of a target can form of a highly energetic growth precursor, resulting in non-equilibrium growth circumstances. As a result, high-quality films can be produced at low substrate temperatures [12]. Laser ablation is a technique for eliminating material from a solid surface by irradiating it with a laser beam. The absorbed laser energy heats the material, which evaporates or sublimates at low laser flux. At high laser flux, the material is frequently converted to plasma. Laser ablation usually refers to removing material using a pulsed laser, while a continuous wave laser beam can ablate material if the laser intensity is high enough. Thin-film machining, material modification, heat treatment, welding, and micro-patterning are only a few examples. Polycomponent materials, on the other hand, can be ablated and deposited onto a substrate in

order to create stoichiometric thin films. This process is known as Pulsed Laser Deposition. In general, the PLD approach is straightforward. During the process, only a few parameters must be controlled. PLD targets are modest in comparison to those employed in other sputtering techniques [13].

Material and methods

The PLD process is used to make Pbs thin films. The experiment was carried out in a vacuum chamber with a 10^{-3} Torr pressure. The target was created as a disk with a diameter of 1cm and a thickness of 0.3cm using a hydraulic piston type (SPECAC) under 6 tons of pressure for 10 minutes using Fluka chemical's PbS. (Germany) These materials were combined with Co element in various amounts with purity (98%) It should be as dense and homogenous as possible to ensure a high-quality deposit. The substrate characteristics are important because they influence the properties of the films formed on it. The effectiveness of substrate cleaning has a big influence on the adherence of deposited films. In this study, glass slides were used to investigate the structural and optical properties of PbS layers and the structural properties measured by XRD , FESEM and AFM , optical properties measured by UV. The laser setup depicts how the substrate and target are positioned within the chamber in relation to the laser beam. The Nd: YAG laser is a type of laser that uses Nd: YAG as its active material (Huafei Tongda Technology- DIAMOND-288 pattern EPLS) Wavelength= 1064 nm, power= 600 m J, frequency= 6 HZ Number of shots = 100 pulses A focused Nd beam's incident beam. The target surface is at a 45° angle.

Result and discussion

XRD diffraction diagnostic results of pure PbS thin films prepared on a glass substrate using Cu – 0.15406nm laser source showed that the crystal system of the film is of cubic system. X-rays with diffraction peaks of the International Center for Diffraction Data (ICDD) number (01 - 078 - 1055) in Figure (1) show the X-ray diffraction pattern (XRD) of pure lead(II) sulfide

before mixing and after mixing with (0.3,0.5,0.7) Co . In pure PbS the high purity and crystallization of the film are visible, which is consistent with the results of the researcher M. Cheraghizade et al. [14]. The diffraction pattern also showed that the high intensity appeared at (2θ˚ =53.6163 and 69.077) and that the dominant trend of growth is (2 2 2) and (1 3 3), respectively. The crystal size (D) of the X-ray diffraction pattern for all samples was calculated using the Debye-Scherer equation and it was found that the crystal size of the Pure PbS sample is (17.74nm).In fig(1) the X-ray diffraction pattern (XRD) of PbS with mixing ratio 0.3Co. The high purity and crystallization of the film are visible. The diffraction pattern also showed that the high intensity appeared at (2θ˚= 79.2234) and that the dominant growth trend is (2 2 0). The diffraction pattern also showed three peaks of Co at (2θ˚ = 45.925, 53.517, and 79.2234), respectively, according to the international standard card number (01 - 088 - 2326). The crystal size of the PbS with mixing 0.3Co sample is (51.3nm). But when mixing PbS with ratio 50% Co. The high purity and crystallization of the film are visible. The diffraction pattern also showed that the high intensity appeared at (2θ˚= 53.5456) and that the dominant growth trend is (2 0 0). The diffraction pattern also showed three peaks of Co at (2θ˚ = 45.925, 53.5456, and 79.1477), respectively, according to the international standard card number (01 - 088 - 2325). The crystal size of the PbS with mixing 0.5Co sample is (55.67nm) . and when PbS mixed with 0.7Co. The high purity and crystallization of the film are visible. The diffraction pattern also showed that the high intensity appeared at (2θ˚= 71.2473) and that the dominant growth trend is (4 2 0). The diffraction pattern also showed four peaks of Co at (2θ˚ = 42.9128, 49.9746, 73.3625, and 88.9283), respectively, according to the international standard card number (96 - 901 - 1627). The crystal size of the PbS with mixed 70% Co sample is (39.57nm).

Academic Science Journal

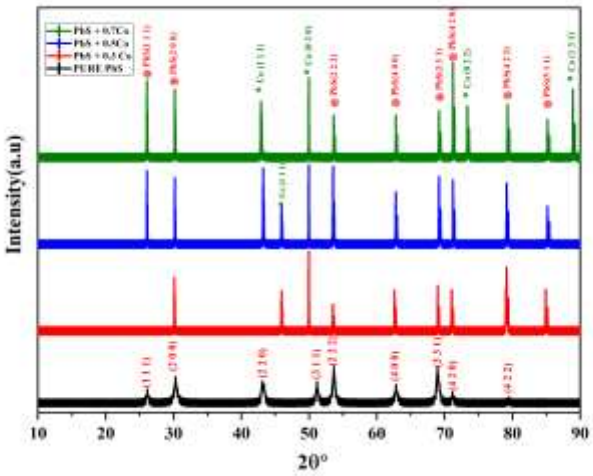

Figure 1: X-ray diffraction pattern of pure PbS and mixed with (0.3,0.5,0.7)Co thin film prepared on a glass substrate

FESEM micrographs of nanocrystalline pure and mixed thin films at low and high magnifications are shown in Figure 2 (a-d). Fig. (2 a) revealed the surface photograph image of pure PbS thin film, it was observed that the film is dense, smooth, non-homogeneous with found pinholes. Also, it was noted that the grains have a mixture of nano non homogeneous and spherical-like shapes with high agglomerated. In addition, it was noted that the PbS thin film formed is high agglomerated. Figure (2 b and c) shows that the mixing ratio of cobalt has a remarkable effect on the surface morphology and grain size of the thin films. Moreover, the images show that the particles were composed of aggregated very small particles. In addition, deposited thin film was dense and smooth, and had few defects and cracks. While the figure (2d) exhibits the mixed thin film with 70% of Co have a un-uniform surface morphology over the entire glass substrate. From images, sparingly packed nano-crystallized which appear to be randomly oriented with irregular and (cauliflower and spherical) shapes of different sizes distribution.

Academic Science Journal

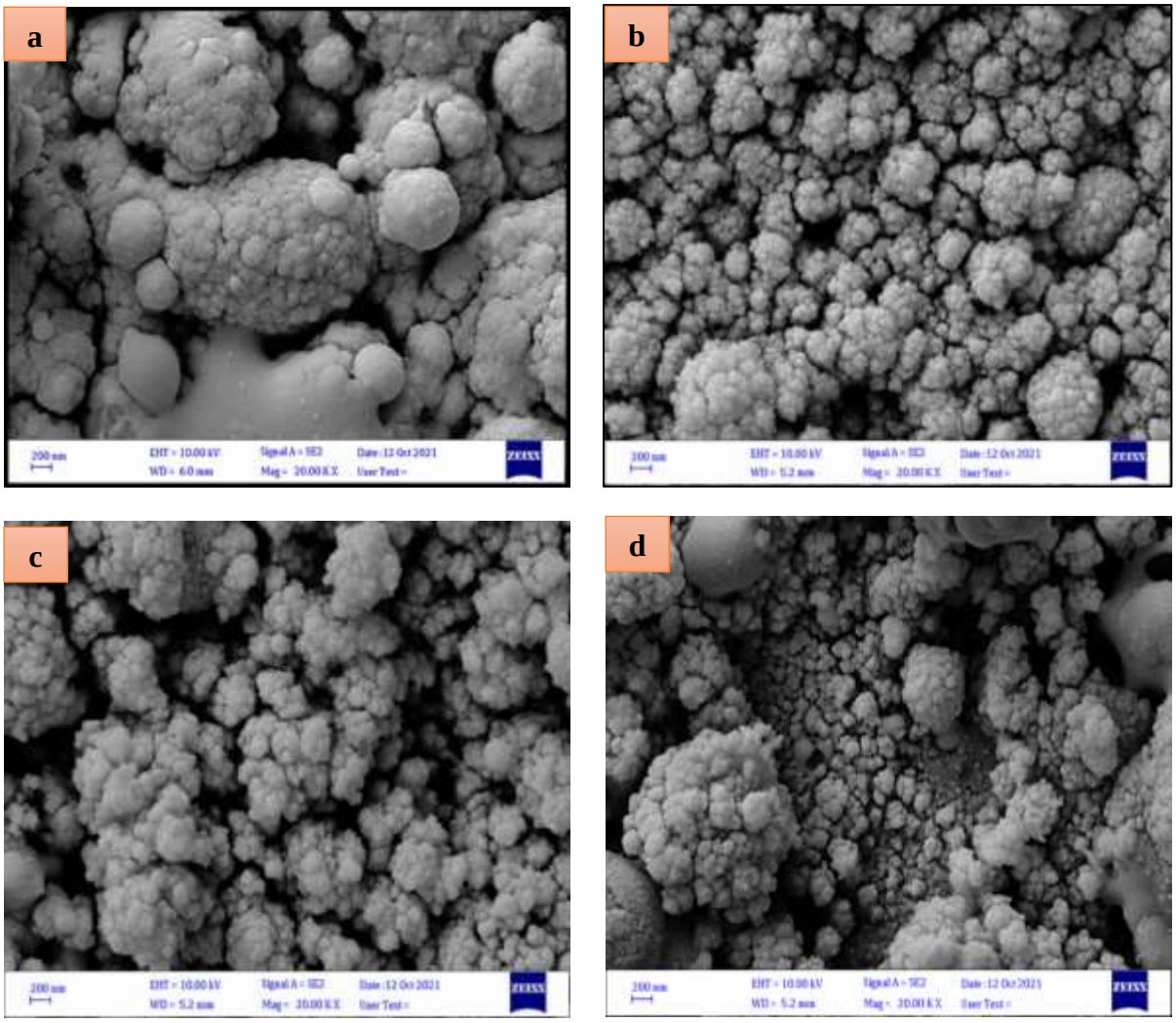

Figure 2: FESEM images of PbS mixed Co thin films at different magnification of (a) pure, (b) 30%, (c) 50% and (d) 70%.

Table 1: Crystallite size of pure and mixed (PbS: Co) thin films.

Samples	Crystallite Size (nm)
PbS	71.2
PbS: 30% Co	68
PbS: 50% Co	74

PbS: 70% Co **80**

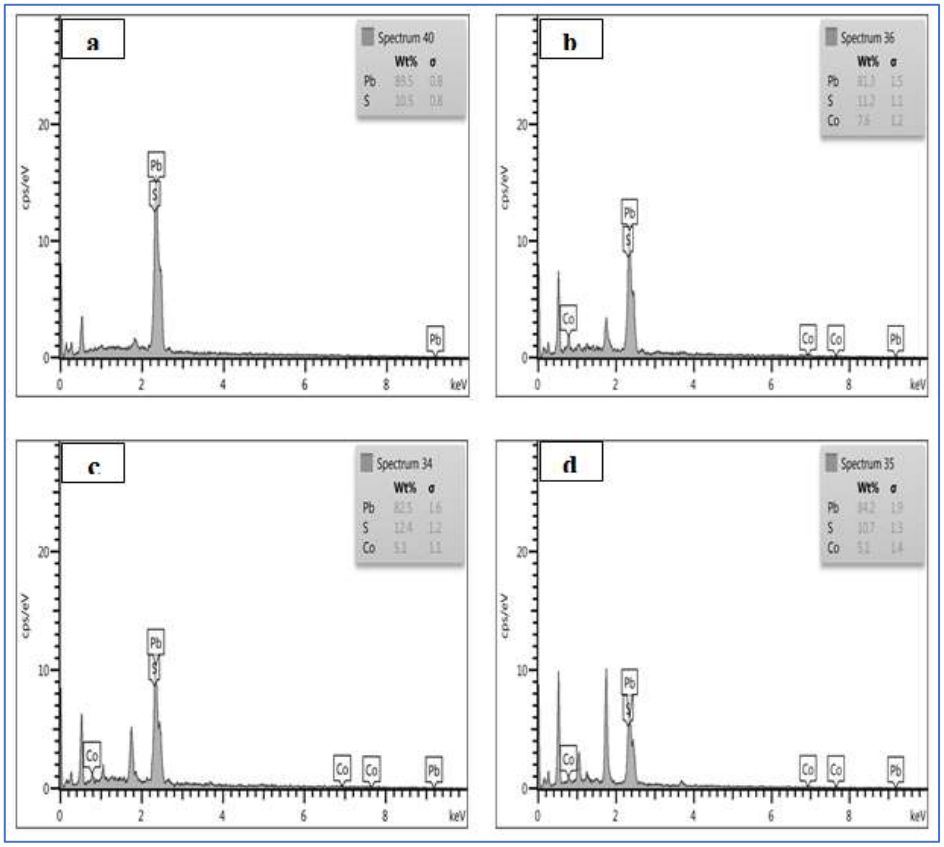

Figure 3: EDS of the pure and PbS mixed Co thin films at (a) pure, (b) 30%, (c) 50% and (d) 70%.

To investigate the chemical composition of pure (PbS) and Co mixed PbS thin films, the elemental analyses of samples were performed by Energy Dispersive X-ray Spectrometer (EDS). Figure 3 (a-d) shows the EDS spectra of un-mixed and mixed films. It was seen that Pb, S and Co were only present in the films, which indicates the purity of all the deposited thin films. The atomic proportions of the elements Pb, S and Co present in the films are presented in table (2).

Table 2: Pb, S and Co concentration in PbS, and PbS: Co samples at various mix ratios.

Sample	Atomic Concentration (%)		
	Pb	S	Co
PbS	89.5	10.5	0
PbS: 30% Co	81.3	11.2	7.6
PbS: 50% Co	82.5	12.4	5.1
PbS: 70% Co	84.2	10.7	5.1

Fig.4 (a-d) represents the 3D AFM images and histogram diagram of pure and mixed films (PbS:Co) with different ratios. The average grain size, average roughness and root mean square (RMS) roughness for prepared films estimated from AFM images, are given in Table (3).

The sample prepared at mix ratio (50%) of Co has highest average grain size, average roughness and RMS roughness of the film. The average diameter values of grain size increase from (36.74 to 303.6) nm with increasing of mix ratio of Co from 0 to 50% then decrease at 70% Co content to 40.66 nm.

Table 3: Surface roughness, root mean square (RMS) and grain size for pure and mixed thin films at different ratios of Co.

Samples	Surface Roughness (nm)	RMS (nm)	Grain Size (nm)
PbS	15.32	18.03	36.74
PbS: 30% Co	20.29	25.71	81.20
PbS: 50% Co	89.63	114.8	303.6
PbS: 70% Co	10.07	13.97	40.66

Academic Science Journal

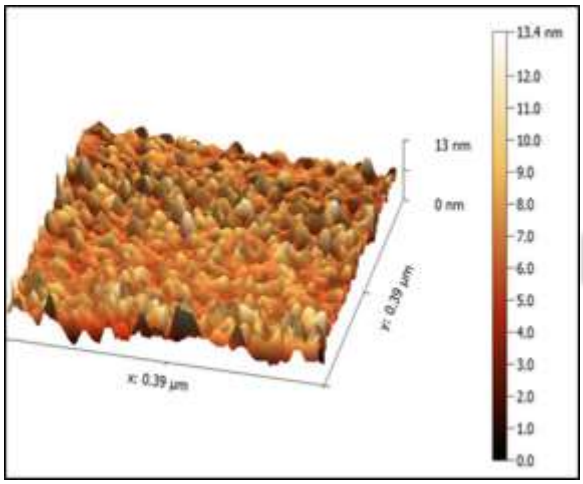

a

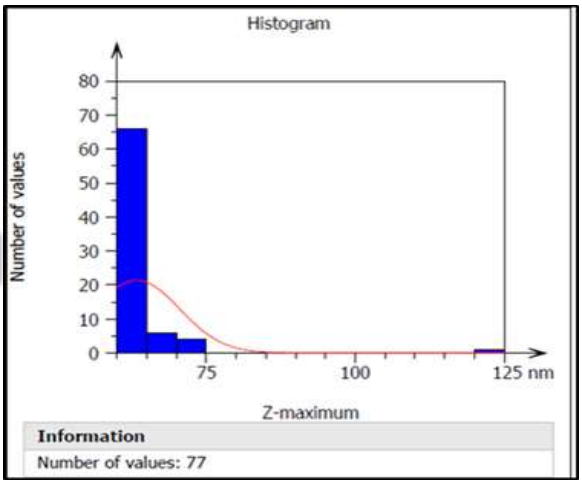

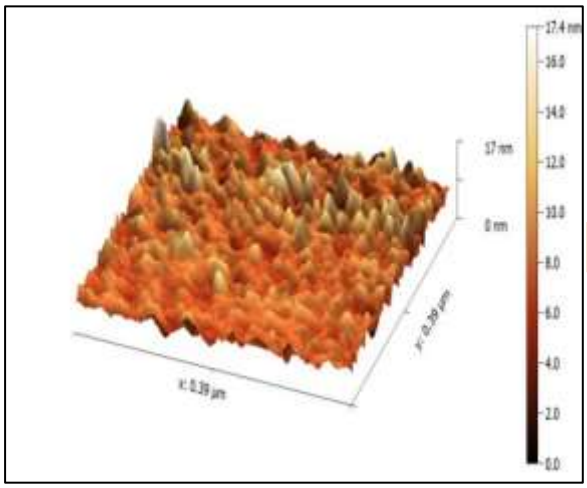

b

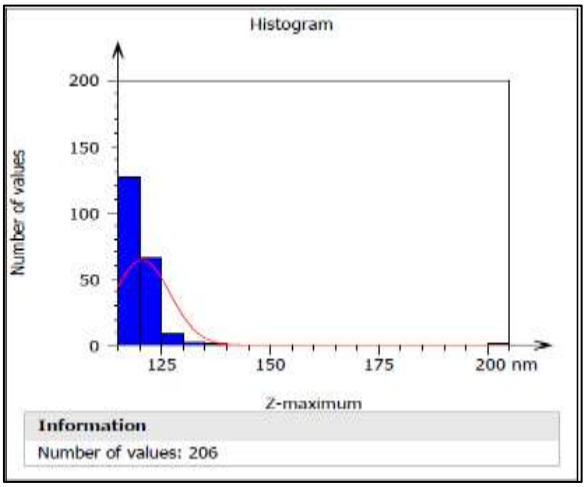

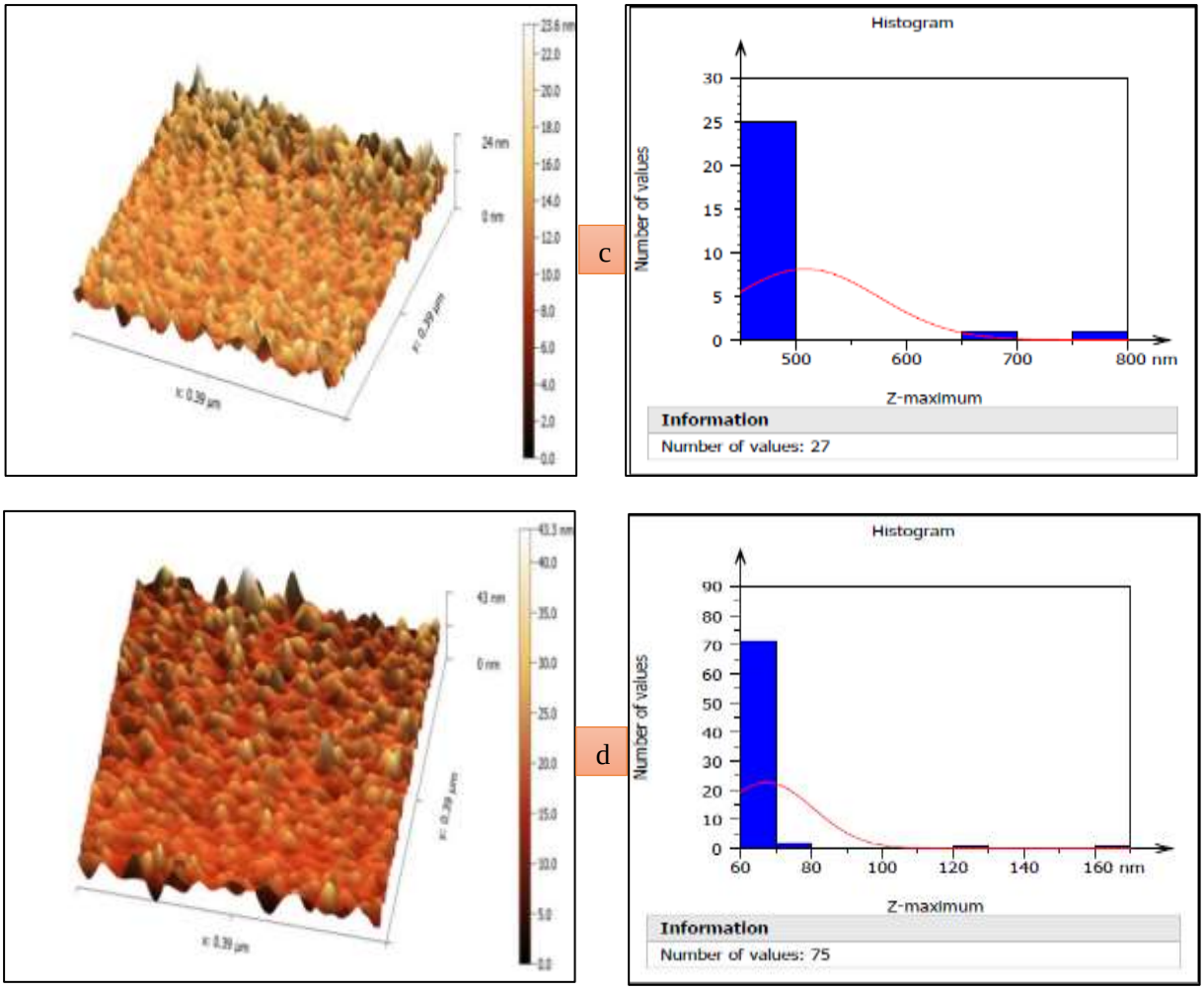

Figure (4): 3D AFM images and histogram for PbS and mixed thin films of different ratios of Co (a) pure, (b) 30%, (c) 50% and (d) 70%.

Figure (5) shows the relation between absorbance and wavelength for pure and mixed thin films. The absorbance is described as a function of the wavelength of prepared thin films, and t the value of the absorbance for prepared samples decreases with increasing wavelength, it is noted that the decrease as highlighted is slight and almost stable for all films prepared at (500 nm)The absorbance shows a broad and strong absorption spectrum at the region of Ultraviolet-visible rays as in Figure (5). The absorption value of prepared films decreases with increasing

wavelength, it is due to the low energy for the incident photons and their inability to irritate electrons from valence band to conduction band, as the relationship between wavelength and photon energy is inverse, this discrepancy in the absorbance values of the prepared films at each wavelength may be due to the different forms of local levels inside the energy gap, which differ according to the nature of the composition and the ratio of the phases formed. In addition, the absorbance of mixed films increase with increase mix ratios of cobalt (Co).

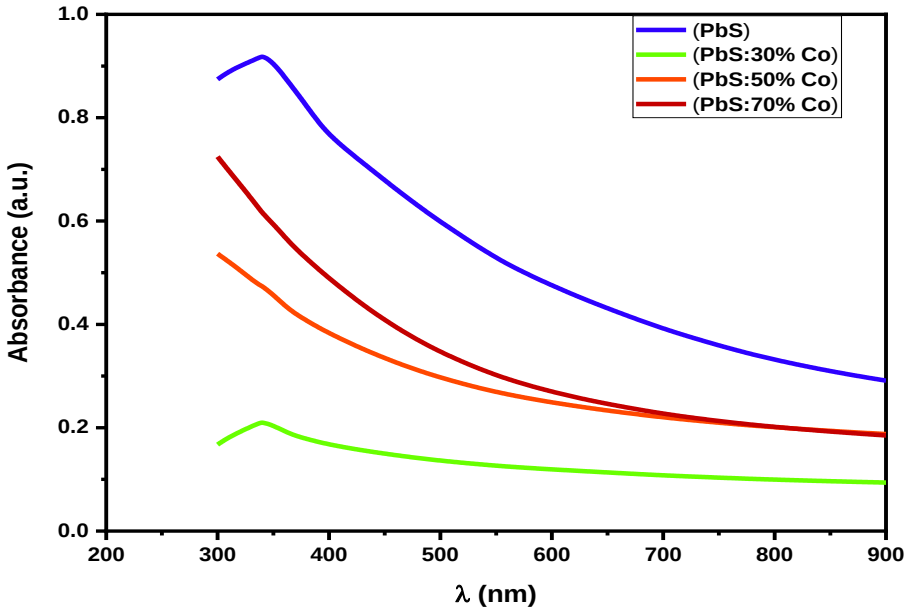

Figure 5: Absorbance versus wavelength of pure and mixed thin films with different ratios of Co.

The absorption coefficient is shown in Figure (6), which shows the change of the absorption coefficient as a function of the incident photon energy for all the prepared films. The results show the slow change of the absorption coefficient at low energies, then the values of the absorption coefficient increase rapidly near the basis absorption edge region of all films. It is noted that the values of the absorption coefficient for all films are (α>104) and this indicates that the electronic transitions are direct transitions, the films have a direct energy gap. It was

found that the value of the absorption coefficient increases with the increase in mix ratios of Co as shown in the figure.

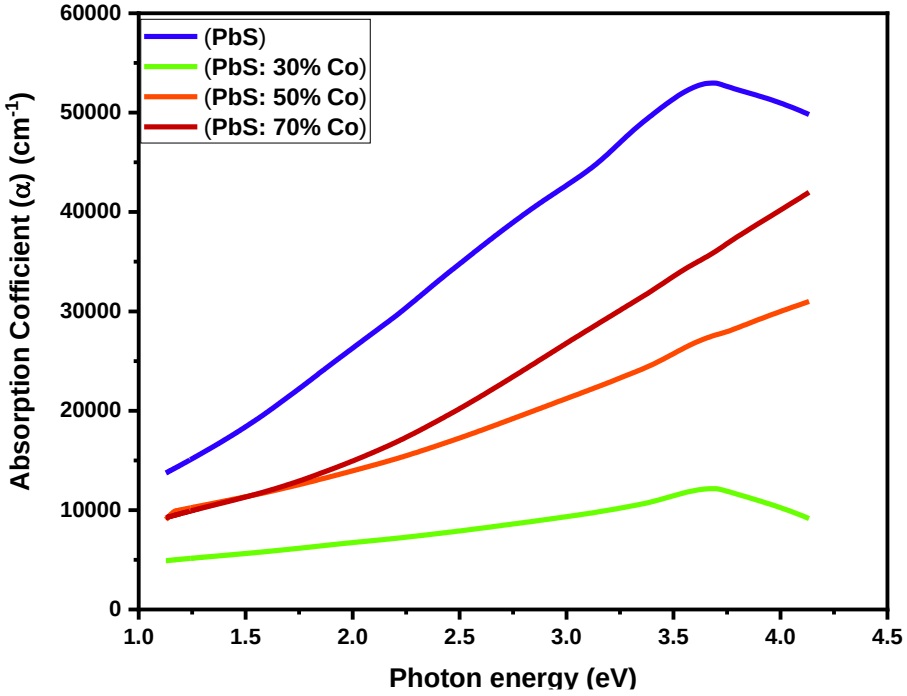

Figure 6: The relation between absorption coefficient and photon energy of pure and mixed thin films at different ratios of Co.

The energy gap can be seen in Figure (7). It is found that the values of the energy band gap of the prepared thin films (pure and mixed) are equal to (2.43 eV) and (2.54, 2.42 and 2.30 eV) and Table (4). it is noted from the results that the energy gap of synthesized films decreases with an increase in mix ratio.

Table 4: Energy gap of pure film and mixed films at various ratios of Co.

Sample	pure	(PbS:30% Co)	(PbS:50% Co)	(PbS:70% Co)
E_g (eV)	2.43	2.54	2.42	2.30

Academic Science Journal

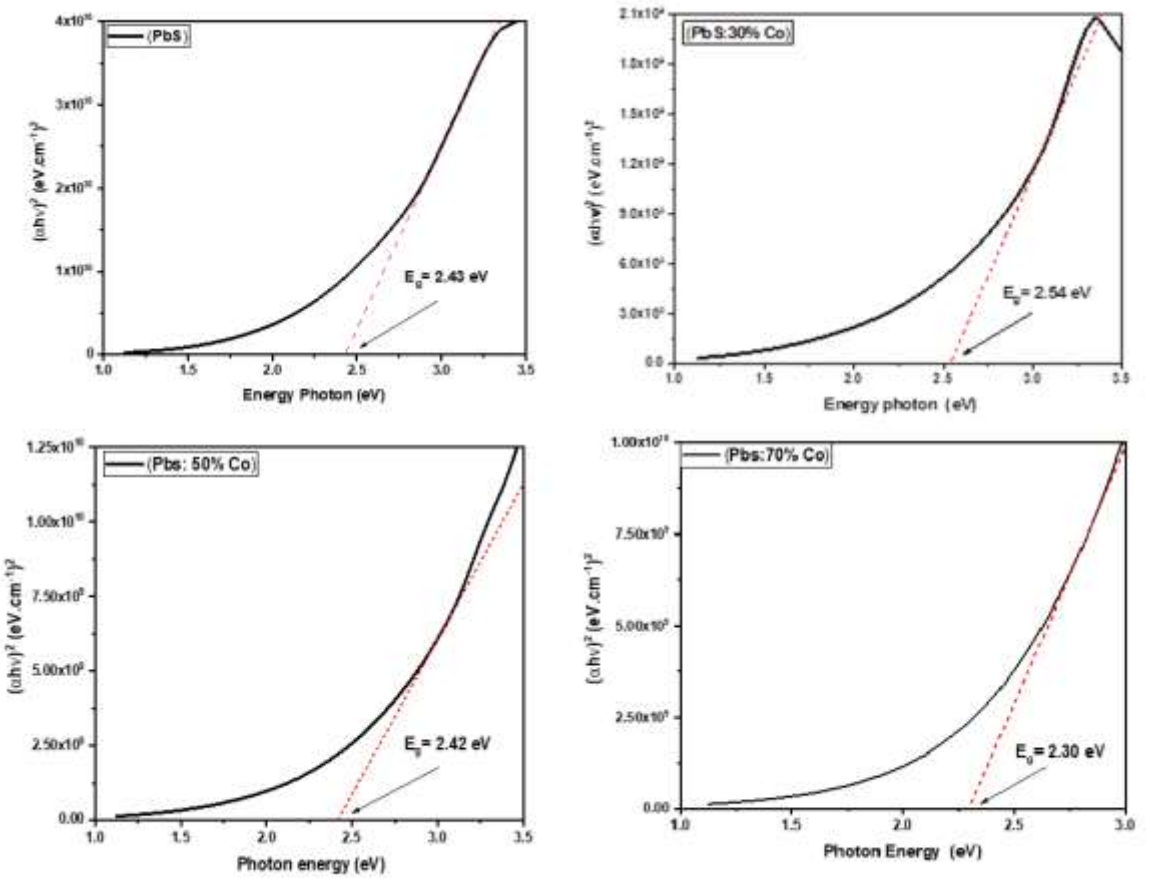

Figure 7: The relation between $(\alpha h\upsilon)^2$ and $(h\upsilon)$ of pure and mixed thin films at different ratios of Co

Hall effect measurement is used to determine the hall mobility (μ_H), carrier concentration (n_H) and majority of electrical carriers type for pure PbS thin films and its mixture with Co at different ratios deposited on glass substrates using laser induce technique at room temperature. The variation of carriers concentration (n_H) and hall mobility (μ_H) of PbS pure and mixed films with (Co) are shown in Table (5). The Hall effect results show that all films are (p-type). From the Table, It was clear that the carrier concentration and carrier mobility (μH) increases with mixing of PbS:Co, This is due to decreasing the disorders of the crystal lattice, as highlighted which causes a decrease in phonon scattering and ionized impurity scattering and results in a

decrease in mobility .In other words, the increase in carrier mobility at mixing PbS:Co is because of the decrease in crystallite size, as shown in the results of the X-ray diffraction analysis .

Table 5: Hall parameters of (PbS) Pure and mixed films with different ratios of Co.

Samples	$R_H \times 10^3$ (cm^3/C)	$n_H \times 10^{15}$ $(cm)^{-3}$	$\mu_H \times 10^3$ ($cm^2/V.sec$)	Type
PbS	**1.45**	**4.29**	**2.68**	**P**
PbS:Co	**7.38**	**8.46**	**46.4**	**P**

Conclusions

Using a pulse laser deposition technique, we were able to create nano-crystalline pure PbS and mixed Co thin films on glass substrates with various Co ratios. All thin films have a cubic structure, according to XRD measurements. Based on optical transmission measurements, the band gap energies for pure PbS and mixed with Co films were determined to be (2.43, 2.54, 2.42,2.30) eV is a crucial material feature that offers up a whole new set of possibilities.

References

1.G. Nabiyouni, R. Sahraei, M. Toghiany, M. H. Majles Ara, K. Hedayati, Rev. Adv. Mater. Sci., 27, 52-57(2011)
2.P. Patnaik, Handbook of Inorganic Chemicals, (The McGraw-Hill Companies ,November, 2001)
3.F. Gode, E. Guneri, F. M. Eman, V. Emir Kafadar, S. Unlu, J. Luminescence, 147, 41–48(2014)
4.S. Seghaier, N. Kamouna, R. Brini, A. B. Amarac, materials Chemistry and Physics, 97, 71-80 (2006)
5.Y. Wang, A. Suna, W. Mahler, R. Kasowski, J. Chem. Phys., 87, 7315– 7319(1987)

6.Rehka Bai, Acta Mater. 131, 11–21(2017)
7.B. Touati, A. Gassoumi, I. Dobryden, M. M. Natile, A. Vomiero, N. K. Turki, Superlattices Microstruct, 97, 519–528(2016)
8.S. Seghaier, N. Kamoun, R. Brini, A.B. Amara, Materials Chemistry and Physics, 97, 71-80(2006)
9.E. Pentia, L. Pintilie, I. Matei, T. Botila, E. Ozbaya, Journal of Optoelectronics and Advanced Materials, 3(2), 525 – 530(2001)
10. V. Popescu, D. Raducanu, G. L. Popescu, Chalcogenide Letters, 9(5), 175 – 183(2012)
11. B. Altıokka, Arabian Journal for Science andEngineering, 40(7), 2085-2093(2015)
12. Dr. Yasmeen, Z. Dawood, S. M. Kadhim, A. Z. Mohammed, 32(9), 1723- 1730(2015)
13. M. C. RAO, International Journal of Modern Physics, Conference Series, Department of Physics, Andhra Loyola College, 22, 355–360(2013)